

Trajectory Tracking for Unmanned Aerial Vehicles with Autopilot in the Loop

Liang Sun¹ and Randal W. Beard²

Abstract—This paper studies the trajectory-tracking strategy for unmanned aerial vehicles where the autopilot is involved in the feedback control. The trajectory-tracking controller is derived based on a generalized design model using Lyapunov based backstepping. The augmentations of the design model and trajectory-tracking controller are conducted to involve the autopilot in the closed-loop system. Lyapunov stability theory is used to guarantee the augmented controller is capable to drive the vehicle to exponentially converge to and follow the desired trajectory with the other states bounded. Simulation results are presented to validate the augmented controller. This paper presents a framework of implementing the developed trajectory-tracking controllers for UAVs without any modification to the autopilot.

I. INTRODUCTION

Unmanned Aerial Vehicles (UAVs) have performed a wide variety of functions in civilian and military applications. Long-endurance, large and costly UAVs like the Global Hawk and the Predator have provided persistent intelligence, surveillance, and reconnaissance (ISR), battle damage assessment, and communications relay capabilities, while smaller and low cost UAVs like the Wasp and the Nighthawk have broadened the scope of potential civil and commercial applications, including environmental monitoring, wilderness search and rescue and forest fire monitoring. For these applications, UAVs are required to be capable of following specific motion patterns. Among the equipments onboard UAVs, the autopilot is a central unit which performs tasks like communicating, state estimation and control. Therefore, almost all the motion control objectives are eventually achieved through the autopilot. However, the specific interface structure of the autopilot makes the developed controller difficult to implement directly because the various design models used to develop controllers may produce different control inputs which may not be compatible with the autopilot interface. In this paper, a strategy of incorporating the autopilot in the controller design for UAV trajectory tracking is present. Lyapunov based backstepping is used to derive the nonlinear time-varying feedback control law.

In the literature, motion control problems for autonomous vehicles can be classified into two categories: path following and trajectory (reference) tracking. Path following problems are primarily concerned with the design of control laws that drive an object (mobile robot, ship, aircraft, etc.) to reach and

follow a geometric path, defined as a function of certain path parameter [1]. The objective of trajectory tracking is to force the actual trajectory of the object to follow a reference signal, a given function of time. The early studies of trajectory tracking for autonomous vehicle can be found in [2], where the feedback linearization and Lyapunov based approaches were employed to develop the control laws for unicycle-type and two-steering-wheels mobile robots to follow a predefined path. The kinematic model of the vehicle was derived with respect to a Frenet-Serret frame which parametrized the vehicles relative to the followed path, in terms of distance and orientation. A detailed review of developments in motion planning and control for nonholonomic system can be found in [3]. The authors summarized the generalized formats of system design models, developed methods for motion planning and the approaches in stabilizing the system using feedback control law. The motion planning and control of a car-trailer system was presented in [4], where the linearization about the desired trajectory was used to convert the nonlinear kinematic model into locally linear equations and LQR based motion control law was developed to achieve the objectives like parallel parking and docking. The study of trajectory tracking for UAVs can be found in [5], where a generalized error dynamics was presented and gain-scheduled control was used to drive the UAV follow a specific path. A motion control strategy for marine craft was presented in [6], where the objectives of both trajectory tracking and path following were combined by using Lagrange multiplier and Lyapunov based backstepping was employed to derive the controller. A similar strategy using Lyapunov based backstepping for trajectory tracking of a hovercraft was presented in [7], [8]. The experimental results was presented in [7]. A motion control strategy accounting for parametric modeling uncertainty was presented in [9], where the Lyapunov based backstepping was used to derive the control law and the experimental results using a hovercraft were presented. A vector field based path following guidance law was presented in [10], [11], where straight line and circle were employed to illustrate the algorithm and Lyapunov stability arguments were also presented.

In the previous studies of motion planning and control for UAVs, most work focused on the derivation of the control laws, while few discussions were presented about the implementation of the control strategy. In the implementing phase of the motion control for UAVs, the relative fixed interface structure of the autopilot may constrain the applicability of the control law. An overview of the autopilots used on small fixed-wing UAVs can be found in [12]. A path following

¹Liang Sun, PhD student in Department of Electrical and Computer Engineering, Brigham Young University, Provo, UT 84602, USA
sun.liang@byu.edu

²Randal W. Beard, Professor in Department of Electrical and Computer Engineering, Brigham Young University, Provo, UT 84602, USA
beard@byu.edu

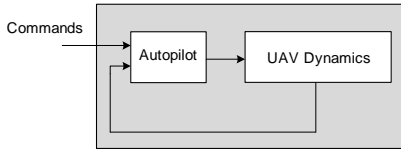


Fig. 1: Closed-loop control in UAVs. The autopilot performs the functions of stabilizing the vehicle as well as following the specific commands.

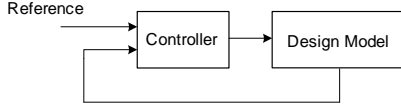


Fig. 2: Closed-loop control system in trajectory tracking controller design.

strategy for UAVs based on adaptive control were presented in [13], [14], which involved autopilot in the closed-loop dynamic. The experimental results were presented in [14] to validate the adaptive controller. In this paper, a preliminary study in trajectory tracking for UAVs with autopilot in the closed-loop system is presented. A time-varying feedback controller is firstly developed using generalized system model. The combined system which involves the autopilot and UAV dynamics in the loop is employed to derive the augmented controller. The UAV trajectory driven by the resulting system is proved exponentially converge to the desired trajectory in the sense of Lyapunov.

The structure of the paper is as follows. Section II presents the formulation of the trajectory tracking problem of UAVs with autopilot in the closed-loop system. In Section III, the derivation of the trajectory tracking control law for the systems with autopilot in the loop is conducted. Section IV shows the numerical results using kinematic and dynamic design models. Finally, Section V summarizes the conclusion.

II. PROBLEM FORMULATION

This section formulates the trajectory tracking problem for UAVs with autopilot in the closed-loop system. A typical closed-loop structure of the feedback stabilization and control in UAVs is shown in Fig. 1, where the autopilot performs the functions of stabilizing the vehicle as well as following the specific commands, including airspeed, attitude angles, angular rate and waypoints. A closed-loop structure of the feedback control for UAVs is shown in Fig. 2, where the design model stands for the equations of motion of UAVs (kinematic or dynamic models) and the controller is designed to achieve specific goals (e.g. trajectory tracking and path following). The outputs of the controller may be various by using different design models and may not be capable of working as the autopilot commands. In order to use the developed controller in Fig. 2 without any modifications to the autopilot, a closed-loop system combining the systems in Fig. 1 and 2 is proposed and shown in Fig. 3, where the design model and controller are augmented to drive the UAV

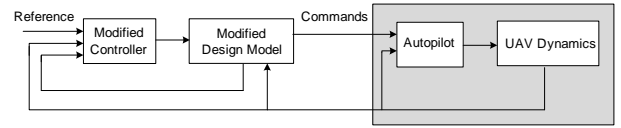


Fig. 3: Closed-loop control system in trajectory tracking with autopilot in the loop. The controller and the design model are modified by feeding back the UAV states and sending the specific commands that autopilot takes.

position exponentially converge to and follow the reference. The main objective of this paper is to develop a strategy of augmenting the design model and the developed controller in Fig. 3 to achieve the trajectory tracking for the UAVs.

III. CONTROL LAW DESIGN FOR TRAJECTORY TRACKING WITH AUTOPILOT IN THE LOOP

This section develops the control law of trajectory tracking for UAVs using the closed-loop system in Fig. 3. Lyapunov based backstepping is employed to derive the controller which is proved to be capable of driving the UAV exponentially converge to and follow the desired trajectory. The controller in Fig. 2 is firstly developed and the controller used in autopilot in Fig. 1 to follow the specific commands is developed after that. Finally, the augmentation law of the controller and design model is developed.

A. Control law design for trajectory tracking using design model

A trajectory tracking control law used in Fig. 2 based on a specific design model is developed in this section.

Lemma 1: *Defining the states $\hat{\eta} \in D_{\eta} \subset \mathbb{R}^3$, $\hat{\xi} \in D_{\xi} \subset \mathbb{R}^3$ and the system inputs $\hat{\mathbf{u}} \in \mathbb{R}^3$, consider the nonlinear system*

$$\dot{\hat{\eta}} = h(\hat{\xi}) \quad (1)$$

$$\dot{\hat{\xi}} = f(\hat{\xi}) + g(\hat{\xi}) \hat{\mathbf{u}} \quad (2)$$

with the assumption that the functions $g(\hat{\xi})$ and $\nabla_h(\hat{\xi}) \triangleq \frac{\partial h}{\partial \hat{\xi}}$ are invertible for $\hat{\xi} \in D_{\xi}$. Suppose that $\eta^d(t)$ is C^2 with bounded time-derivatives. If constants \hat{k}_1 and \hat{k}_2 are positive, and $\hat{\mathbf{u}}$ is selected as

$$\begin{aligned} \hat{\mathbf{u}} = & \left(\nabla_h(\hat{\xi}) g(\hat{\xi}) \right)^{-1} \left(\ddot{\eta}^d - \nabla_h(\hat{\xi}) f(\hat{\xi}) \right. \\ & - \left(\hat{k}_1 + \hat{k}_2 \right) \left(\dot{\hat{\eta}} - \dot{\eta}^d \right) \\ & \left. - \left(1 + \hat{k}_1 \hat{k}_2 \right) \left(\hat{\eta} - \eta^d \right) \right), \end{aligned} \quad (3)$$

then tracking error $\hat{\eta} - \eta^d$ exponentially converges to the origin with bounded $\hat{\xi}$.

Proof:

Step 1: Convergence of $\hat{\eta} \rightarrow \eta^d$.

Let $\mathbf{e}_{\hat{\eta}} \triangleq \hat{\eta} - \eta^d$ be the tracking error and the error dynamics is given by $\dot{\mathbf{e}}_{\hat{\eta}} = \dot{\hat{\eta}} - \dot{\eta}^d$. Define the Lyapunov function

candidate $V_1 = \frac{1}{2} \mathbf{e}_{\hat{\eta}}^T \mathbf{e}_{\hat{\eta}}$, which has the time derivative

$$\begin{aligned} \dot{V}_1 &= \mathbf{e}_{\hat{\eta}}^T \dot{\mathbf{e}}_{\hat{\eta}} \\ &= \mathbf{e}_{\hat{\eta}}^T (\dot{\hat{\eta}} - \dot{\eta}^d). \end{aligned} \quad (4)$$

At this stage of the development, we consider $\dot{\hat{\eta}}$ as a virtual control, where \dot{V}_1 can be made negative definite by setting $\dot{\hat{\eta}}$ equals to $\dot{\eta}^d - \hat{k}_1 \mathbf{e}_{\hat{\eta}}$. Introducing the error variable

$$\mathbf{z} \triangleq \dot{\eta}^d - \hat{k}_1 \mathbf{e}_{\hat{\eta}} - \dot{\hat{\eta}} \quad (5)$$

and adding and subtracting \mathbf{z} in (4) gives

$$\dot{V}_1 = -\hat{k}_1 \mathbf{e}_{\hat{\eta}}^T \mathbf{e}_{\hat{\eta}} - \mathbf{e}_{\hat{\eta}}^T \mathbf{z}.$$

Consider the augmented Lyapunov function candidate

$$V_2 \triangleq V_1 + \frac{1}{2} \mathbf{z}^T \mathbf{z}$$

with the time derivative

$$\begin{aligned} \dot{V}_2 &= -\hat{k}_1 \mathbf{e}_{\hat{\eta}}^T \mathbf{e}_{\hat{\eta}} + \mathbf{z}^T (-\mathbf{e}_{\hat{\eta}} + \dot{\mathbf{z}}) \\ &= -\hat{k}_1 \mathbf{e}_{\hat{\eta}}^T \mathbf{e}_{\hat{\eta}} \\ &\quad + \mathbf{z}^T (-\mathbf{e}_{\hat{\eta}} + \dot{\eta}^d - \hat{k}_1 \dot{\mathbf{e}}_{\hat{\eta}} - \nabla_h (f + g\hat{\mathbf{u}})). \end{aligned}$$

If $\hat{\mathbf{u}}$ is given by (3), the time derivative of V_2 becomes

$$\dot{V}_2 = -\hat{k}_1 \mathbf{e}_{\hat{\eta}}^T \mathbf{e}_{\hat{\eta}} - \hat{k}_2 \mathbf{z}^T \mathbf{z}.$$

Based on Lyapunov stability theory, it can concluded that $\mathbf{e}_{\hat{\eta}}$ and \mathbf{z} exponentially converge to the origin.

Step 2: Boundedness of $\hat{\xi}$.

Because

$$\mathbf{z} = \dot{\eta}^d - \hat{k}_1 \mathbf{e}_{\hat{\eta}} - h(\hat{\xi})$$

and $\mathbf{e}_{\hat{\eta}}$ and \mathbf{z} exponentially converge to the origin, it can be concluded that $h(\hat{\xi})$ exponentially converges to $\dot{\eta}^d$. Because $\dot{\eta}^d$ is bounded, then $h(\hat{\xi})$ is bounded, which implies that its time derivative $\frac{dh}{dt} = \nabla_h(\hat{\xi}) \dot{\hat{\xi}}$ is bounded. Meanwhile, $\nabla_h(\hat{\xi})$ is invertible and is also bounded, then $\dot{\hat{\xi}} = \nabla_h^{-1} \frac{dh}{dt}$ is bounded. \square

B. Feedback control in autopilot

A feedback control law for autopilot to follow the desired commands, shown in Fig. 1, is developed in this section. The commands are selected as $\hat{\xi}$ in this paper.

Lemma 2: *Defining the states $\xi \in D_\xi \subset \mathbb{R}^3$ and system inputs $\mathbf{u} \in \mathbb{R}^3$, consider the nonlinear system*

$$\dot{\xi} = f(\xi) + g(\xi) \mathbf{u},$$

with the assumption that the function $g(\mathbf{x})$ is invertible for \mathbf{x} on D_ξ . Suppose that $\hat{\xi}(t) \in D_\xi$ is C^2 with bounded time-derivatives. If constant k is positive, and \mathbf{u} is selected as

$$\mathbf{u} = g(\hat{\xi})^{-1} \left(-f(\hat{\xi}) + \dot{\hat{\xi}} - k(\hat{\xi} - \hat{\xi}) \right), \quad (6)$$

then the tracking error $\xi - \hat{\xi}$ exponentially converges to the origin.

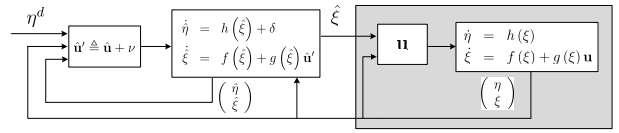


Fig. 4: Closed-loop control system for trajectory tracking with autopilot in the loop using a specific equations of motion. The commands sent to the autopilot are selected as $\hat{\xi}$.

Proof:

Let $\mathbf{e}_\xi \triangleq \xi - \hat{\xi}$ and the error dynamic is given by $\dot{\mathbf{e}}_\xi = \dot{\xi} - \dot{\hat{\xi}}$. Define the Lyapunov function candidate $V_3 = \frac{1}{2} \mathbf{e}_\xi^T \mathbf{e}_\xi$, which has the time derivative

$$\begin{aligned} \dot{V}_3 &= \mathbf{e}_\xi^T \dot{\mathbf{e}}_\xi \\ &= \mathbf{e}_\xi^T (f + g\mathbf{u} - \dot{\hat{\xi}}). \end{aligned} \quad (7)$$

If \mathbf{u} is given by (6), the time derivative of V_3 becomes

$$\dot{V}_3 = -k \mathbf{e}_\xi^T \mathbf{e}_\xi.$$

Based on Lyapunov stability theory, it can concluded that \mathbf{e}_ξ exponentially converges to the origin. \square

C. Control law design for combined system

A control strategy, shown in Fig. 3, by augmenting the design model and controller developed in Lemma 1 is presented in this section. The UAV dynamics are selected as the copy of the design model, and the autopilot control law is selected as the one developed in Lemma 2. The combined systems using specific equations of motion are shown in Fig. 4. The commands sent to the autopilot are selected as $\hat{\xi}$.

Theorem 1: *Defining the states $\hat{\eta}, \eta \in D_\eta \subset \mathbb{R}^3$, $\hat{\xi}, \xi \in D_\xi \subset \mathbb{R}^3$, and the system inputs $\hat{\mathbf{u}}^l, \mathbf{u} \in \mathbb{R}^3$, consider the nonlinear systems described in Fig. 4 with the assumption that the functions $g(\mathbf{x})$ and $\nabla_h(\mathbf{x}) \triangleq \frac{\partial h}{\partial \mathbf{x}}$ are invertible for \mathbf{x} on D_ξ . Suppose that $\eta^d(t)$ is C^2 with bounded time-derivatives. If constants \hat{k}_1, \hat{k}_2 and L are positive, δ is selected as $L(\eta - \hat{\eta})$, $\hat{\mathbf{u}}$ is selected in (3), \mathbf{u} is selected in (6) and ν is selected as*

$$\nu = - \left(\nabla_h(\hat{\xi}) g(\hat{\xi}) \right)^{-1} (\dot{\delta} + \hat{k}_2 \delta), \quad (8)$$

then the tracking error $\eta - \eta^d$ and $\hat{\eta} - \eta^d$ exponentially converge to the origin with bounded ξ and $\hat{\xi}$.

Proof:

Step 1: Convergence of $\xi \rightarrow \hat{\xi}$.

This can be proved by Lemma 2.

Step 2: Convergence of $\eta \rightarrow \hat{\eta}$.

Let $\tilde{\mathbf{e}}_\eta \triangleq \eta - \hat{\eta}$ and the error dynamic of $\tilde{\mathbf{e}}_\eta$ is given by

$$\begin{aligned} \dot{\tilde{\mathbf{e}}}_\eta &= \dot{\eta} - \dot{\hat{\eta}} \\ &= h(\xi) - h(\hat{\xi}) - L\tilde{\mathbf{e}}_\eta. \end{aligned}$$

Because ξ exponentially converges to $\hat{\xi}$, it can be concluded that $h(\xi)$ exponentially converges to $h(\hat{\xi})$. Because L is a positive constant, it can be concluded that the tracking error \tilde{e}_η exponentially converges to the origin by using the input-to-state stability theory [15].

Step 3: Convergence of $\hat{\eta} \rightarrow \eta^d$:

Let $\mathbf{e}_{\hat{\eta}} \triangleq \hat{\eta} - \eta^d$ and the error dynamic of $\dot{\mathbf{e}}_{\hat{\eta}}$ is given by $\dot{\mathbf{e}}_{\hat{\eta}} = \dot{\hat{\eta}} - \dot{\eta}^d$. Define the Lyapunov function candidate $V_4 \triangleq \frac{1}{2} \mathbf{e}_{\hat{\eta}}^T \mathbf{e}_{\hat{\eta}}$, which has the time derivative

$$\begin{aligned} \dot{V}_4 &= \mathbf{e}_{\hat{\eta}}^T (\dot{\hat{\eta}} - \dot{\eta}^d) \\ &= \mathbf{e}_{\hat{\eta}}^T \left(h(\hat{\xi}) + \delta - \dot{\eta}^d \right). \end{aligned} \quad (9)$$

Introducing the error variable

$$\hat{\mathbf{z}} \triangleq -h(\hat{\xi}) - \delta + \dot{\eta}^d - \hat{k}_1 \mathbf{e}_{\hat{\eta}}$$

and adding and subtracting $\hat{\mathbf{z}}$ in (9) gives

$$\dot{V}_4 = -\hat{k}_1 \mathbf{e}_{\hat{\eta}}^T \mathbf{e}_{\hat{\eta}} - \mathbf{e}_{\hat{\eta}}^T \hat{\mathbf{z}}.$$

Consider the augmented Lyapunov function candidate

$$V_5 \triangleq V_4 + \frac{1}{2} \hat{\mathbf{z}}^T \hat{\mathbf{z}}$$

with time derivative

$$\begin{aligned} \dot{V}_5 &= -\hat{k}_1 \mathbf{e}_{\hat{\eta}}^T \mathbf{e}_{\hat{\eta}} + \hat{\mathbf{z}}^T \left(-\mathbf{e}_{\hat{\eta}} + \dot{\hat{\mathbf{z}}} \right) \\ &= -\hat{k}_1 \mathbf{e}_{\hat{\eta}}^T \mathbf{e}_{\hat{\eta}} + \hat{\mathbf{z}}^T \left(-\mathbf{e}_{\hat{\eta}} + \dot{\eta}^d - \hat{k}_1 \dot{\mathbf{e}}_{\hat{\eta}} \right. \\ &\quad \left. - \dot{\delta} - \nabla_h \left(h(\hat{\xi}) \right) \left(f(\hat{\xi}) + g(\hat{\xi}) (\hat{\mathbf{u}} + \nu) \right) \right) \end{aligned}$$

If $\hat{\mathbf{u}}$ is selected in (3) and ν is selected in (8), it can be obtained

$$\dot{V}_5 = -\hat{k}_1 \mathbf{e}_{\hat{\eta}}^T \mathbf{e}_{\hat{\eta}} - \hat{k}_2 \hat{\mathbf{z}}^T \hat{\mathbf{z}}.$$

Based on Lyapunov stability theorem [15] it can be concluded that $\mathbf{e}_{\hat{\eta}}$ exponentially converges to the origin.

Step 4: Boundedness of ξ and $\hat{\xi}$.

Because

$$\dot{\hat{\mathbf{z}}} = -h(\hat{\xi}) - \delta + \dot{\eta}^d - \hat{k}_1 \mathbf{e}_{\hat{\eta}},$$

and δ exponentially converges to the origin, it can be proved that $\hat{\xi}$ is bounded by using the similar strategy in Lemma 1. From Lemma 2, it can be concluded that ξ exponentially converges to $\hat{\xi}$, so ξ is also bounded.

IV. NUMERICAL RESULTS

In this section, simulation results are shown to validate the augmented controller developed in the previous section. Both the kinematic and dynamic models are employed to validate the controllers. The reference trajectory is selected as an inclined circular orbit. Letting R be the desired orbit radius in the horizontal plane, V_d be the desired constant ground speed, h_0 be the desired average altitude and h_c be the desired magnitude of the altitude oscillation, the reference trajectory η^d in North-East-Down (NED) frame is given by

$$\eta^d(t) = \begin{pmatrix} R \sin(\omega_0 t) \\ R \cos(\omega_0 t) \\ -h_0 + h_c \sin(\omega_0 t) \end{pmatrix},$$

TABLE I: Initial configuration of the system

Item	UAV Dynamics	Design Model
\mathbf{p}_0 , m	(0, 260, -180)	(0, 220, -150)
V_{a0} , m/s	20	12
ψ_0 , rad	$\frac{\pi}{2}$	π
γ_{a0} , rad	0	0
ϕ_0 rad	0	0

where $\omega_0 = V_d/R$. In this paper, R is selected as 200 m, V_d is selected as 14 m/s, h_0 is selected as 200 m and h_c is selected as 10 m.

A. Simulation results using kinematic model

Letting $(p_n, p_e, p_d)^T$ be the position of the UAV in NED frame, V_a be the airspeed, ψ be the heading angle, $(w_n, w_e, w_d)^T$ be the constant wind vector in NED frame, and airspeed rate u_{V_a} , heading angular rate u_ψ and flight path angular rate u_{γ_a} be the control inputs, the equations of motion of the UAV can be written as

$$\dot{p}_n = V_a \cos \psi \cos \gamma_a + w_n \quad (10)$$

$$\dot{p}_e = V_a \sin \psi \cos \gamma_a + w_e \quad (11)$$

$$\dot{p}_d = -V_a \sin \gamma_a + w_d \quad (12)$$

$$\dot{V}_a = u_{V_a} \quad (13)$$

$$\dot{\psi} = u_\psi \quad (14)$$

$$\dot{\gamma}_a = u_{\gamma_a}. \quad (15)$$

Comparing (10) to (15) with the equations in Fig. 4, it can be obtained that $\hat{\eta} = (p_n, p_e, p_d)^T$, $\hat{\xi} = (V_a, \psi, \gamma_a)^T$, $\hat{\mathbf{u}} = (u_{V_a}, u_\psi, u_{\gamma_a})^T$, $f(\cdot) = 0$, $g(\cdot) = \mathbf{I}_3$ and

$$h(\cdot) = \begin{pmatrix} V_a \cos \psi \cos \gamma_a + w_n \\ V_a \sin \psi \cos \gamma_a + w_e \\ -V_a \sin \gamma_a + w_d \end{pmatrix}.$$

In the simulation, the control gains are selected as $k = 2$, $\hat{k}_1 = 0.5$, $\hat{k}_2 = 2$ and $L = 1$. Letting the initial position, airspeed, heading angle and flight path angle of the UAV be \mathbf{p}_0 , V_{a0} , ψ_0 and γ_{a0} , respectively, the initial configuration of the system in the simulation is listed in Table I. Without loss of generality The constant wind vector is selected as $(3, 0, 0)^T$ m/s. The performance limits of the UAV are selected as $\dot{\psi} \in [-40, 40]$ deg/s, $V_a \in [10, 20]$ m/s, $\gamma_a \in [-15, 15]$ deg and $\phi \in [-35, 35]$ deg.

The simulation results are shown in Fig. 5. The UAV trajectories in the 3-D and top-down views are shown in Fig. 5 (a) and (b), respectively. It can be seen that the actual trajectory of the UAV started from a position outside the desired orbit with an initial distance error approximately 60 m and converged to the desired trajectory after approximately a half circle. Fig. 5 (c) shows the tracking error between the UAV trajectory and the reference in North, East, and altitude directions. It can be seen that all the errors converged to zero after 40 s. Fig. 5 (d) shows the evolution of the states V_a , ψ and γ_a . The oscillation of V_a explains the presence of wind and the oscillation of γ_a matched the desired altitude oscillation.

B. Simulation results using dynamic model

Although models that include kinematic relationships may be suitable for certain control objectives, models that include dynamic effects are required for other purposes. Letting m be the UAV mass, g be the gravitational constant at Earth sea level, L and D be the aerodynamic lift and drag forces, respectively, ϕ be the roll angle, the control inputs be the thrust u_τ , the load factor $u_n \triangleq \frac{L}{mg}$ and roll angular rate u_ϕ , the dynamic model of the UAV can be written as

$$\dot{p}_n = V_a \cos \psi \cos \gamma_a + w_n \quad (16)$$

$$\dot{p}_e = V_a \sin \psi \cos \gamma_a + w_e \quad (17)$$

$$\dot{p}_d = -V_a \sin \gamma_a + w_d \quad (18)$$

$$\dot{V}_a = \frac{u_\tau - D}{m} - g \sin \gamma_a \quad (19)$$

$$\dot{\psi} = \frac{L \sin \phi}{m V_a \cos \gamma_a} \quad (20)$$

$$\dot{\gamma}_a = \frac{g}{V_a} (u_n \cos \phi - \cos \gamma_a) \quad (21)$$

$$\dot{\phi} = u_\phi. \quad (22)$$

To match the UAV dynamic model to 1 and 2, Equation (19) through (21) are rearranged as

$$\begin{pmatrix} \dot{V}_a \\ \dot{\gamma}_a \\ \dot{\psi} \end{pmatrix} = \begin{pmatrix} -\frac{D}{m} - g \sin \gamma_a \\ -\frac{g}{V_a} \cos \gamma_a \\ 0 \end{pmatrix} + \begin{pmatrix} \frac{1}{m} & 0 & 0 \\ 0 & \frac{g}{V_a} \cos \phi & 0 \\ 0 & 0 & \frac{L}{m V_a \cos \gamma_a} \end{pmatrix} \begin{pmatrix} u_\tau \\ u_n \\ \mu \end{pmatrix},$$

where $\mu \triangleq \sin \phi$ is the virtual control input. Then it can be obtained that

$$f(\cdot) = \begin{pmatrix} -\frac{D}{m} - g \sin \gamma_a \\ -\frac{g}{V_a} \cos \gamma_a \\ 0 \end{pmatrix}$$

$$g(\cdot) = \begin{pmatrix} \frac{1}{m} & 0 & 0 \\ 0 & \frac{g}{V_a} \cos \phi & 0 \\ 0 & 0 & \frac{L}{m V_a \cos \gamma_a} \end{pmatrix}$$

$$\hat{\mathbf{u}}' = \begin{pmatrix} u_\tau \\ u_n \\ \mu \end{pmatrix}$$

Then the roll angular rate can be calculated by $u_\phi = (\sin^{-1}(\hat{\mathbf{u}}'(3)) - \phi) / T_s$, where T_s is the sample time of the simulation.

In the simulation, the control gains are selected as $k = 2$, $\hat{k}_1 = 0.2$, $\hat{k}_2 = 0.5$, $L = 0.5$. Letting the initial roll angle be ϕ_0 , the initial configuration of the system in the simulation is listed in Table I. The constant wind vector is selected as $(3, 0, 0)^T$ m/s.

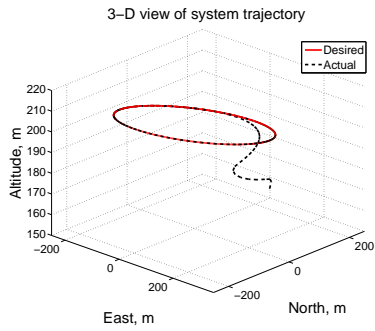
The simulation results are shown in Fig. 6 which was very similar to the results using a kinematic model shown in Fig. 5. It can be seen that the convergence of the actual trajectory was slightly slower than that in Fig. 5. The oscillation of the roll angle explained the presence of wind.

V. CONCLUSION

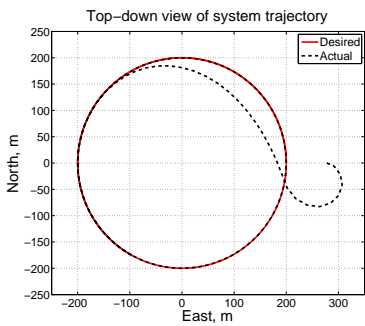
This paper presented a trajectory tracking strategy for UAVs with autopilot in the closed-loop system. Lyapunov based backstepping was used to derive the trajectory-tracking controller using a design model with generalized equations of motion. To involve the autopilot in the closed-loop system, the developed trajectory-tracking controller and the design model were augmented. The updated controller was also proved using Lyapunov stability theory to be capable of driving the vehicle to exponentially converge to and follow the reference by keeping the other states bounded. The simulations using both kinematic and dynamic models were conducted to validate the developed controllers. The numerical results showed that the augmented controller was capable to achieve the trajectory-tracking objectives.

REFERENCES

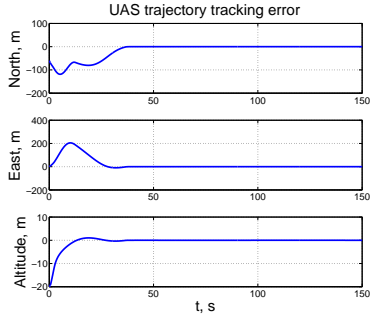
- [1] P. Aguiar, D. Dačić, J. Hespanha, and P. Kokotović, "Path-following or reference-tracking? An answer relaxing the limits to performance," in *IAV2004, 5th IFAC/EURON Symposium on Intelligent Autonomous Vehicles*, Lisbon, Portugal, 2004.
- [2] A. Micaelli and C. Samson, "Trajectory tracking for unicycle-type and two-steering-wheels mobile robots," The French National Institute for Research in Computer Science and Control, Sophia-Antipolis, France, Technical Report 2097, 1993.
- [3] I. Kolmanovsky and N. H. McClamroch, "Developments in nonholonomic control problems," *IEEE Control Systems*, vol. 15, no. 6, pp. 20–36, Dec. 1995.
- [4] A. W. Divilbiss and J. T. Wen, "Trajectory tracking control of a car-trailer system," *IEEE Transactions on Control Systems Technology*, vol. 5, no. 3, pp. 269–278, May 1997.
- [5] I. Kaminer, A. Pascoal, E. Hallberg, and C. Silvestre, "Trajectory tracking for autonomous vehicles: An integrated approach to guidance and control," *AIAA Journal of Guidance, Control and Dynamics*, vol. 21, no. 1, pp. 29–38, 1998.
- [6] P. Encarnação and A. Pascoal, "Combined trajectory tracking and path following for marine craft." Orlando, FL: the IEEE Conference on Decision and Control, 2001, pp. 964–969.
- [7] A. P. Aguiar, L. Cremean, and J. P. Hespanha, "Position tracking for a nonlinear underactuated hovercraft: controller design and experimental results," in *Proc. 42nd IEEE Conference on Decision and Control*, vol. 4, 9–12 Dec. 2003, pp. 3858–3863.
- [8] A. P. Aguiar and J. P. Hespanha, "Position tracking of underactuated vehicles," in *Proc. American Control Conference the 2003*, vol. 3, 4–6 June 2003, pp. 1988–1993.
- [9] —, "Trajectory-tracking and path-following of underactuated autonomous vehicles with parametric modeling uncertainty," *IEEE Transactions on Automatic Control*, vol. 52, no. 8, pp. 1362–1379, August 2007.
- [10] D. R. Nelson, D. B. Barber, T. W. McLain, and R. W. Beard, "Vector field path following for miniature air vehicles," *IEEE Transactions on Robotics*, vol. 37, pp. 519–529, June 2007.
- [11] R. W. Beard and T. W. McLain, *Small Unmanned Aircraft: Theory and Practice*. Princeton University Press, 2012.
- [12] H. Chao, Y. Cao, and Y. Chen, "Autopilots for small fixed-wing unmanned air vehicles: A survey," in *Proceedings of the 2007 IEEE International Conference on Mechatronics and Automation*, Harbin, China, August 2007.
- [13] I. Kaminer, A. Pascoal, E. Xargay, N. Hovakimyan, C. Cao, and V. Dobrokhodov, "Path following for unmanned aerial vehicles using l1 adaptive augmentation of commercial autopilots," *Journal of Guidance Control and Dynamics*, vol. 33, no. 2, pp. 550–564, 2010.
- [14] V. Dobrokhodov, I. Kaminer, I. Kitsios, E. Xargay, N. Hovakimyan, C. Cao, I. M. Gregory, and L. Valavani, "Experimental validation of l1 adaptive control: The rohms counterexample in flight," *Journal of Guidance Control and Dynamics*, vol. 34, no. 5, pp. 1311–1328, 2011.
- [15] H. K. Khalil, *Nonlinear Systems*, 3rd ed. Upper Saddle River, NJ: Prentice Hall, 2002.



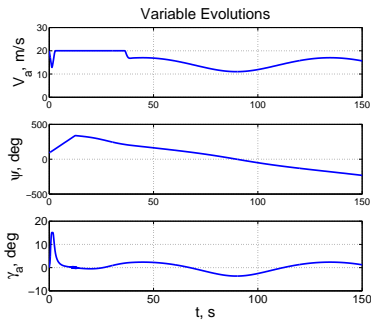
(a) 3-D view of system trajectory.



(b) Top-down view of system trajectory.

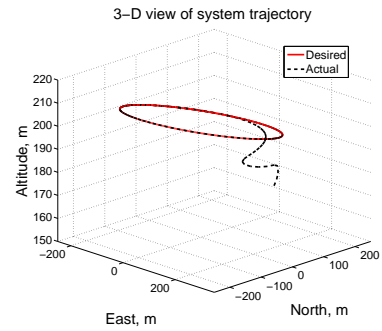


(c) Trajectory tracking errors.

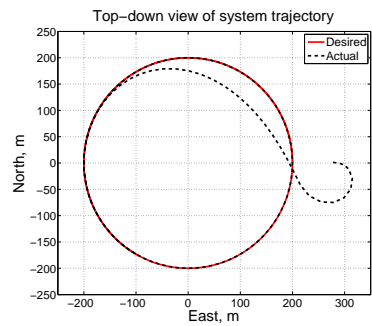


(d) Evolution of the states.

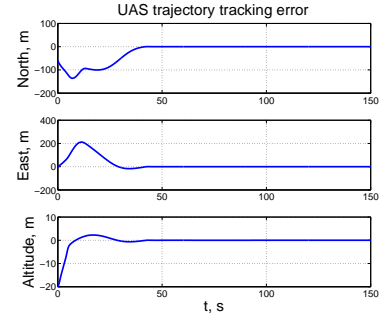
Fig. 5: Simulation results using kinematic model.



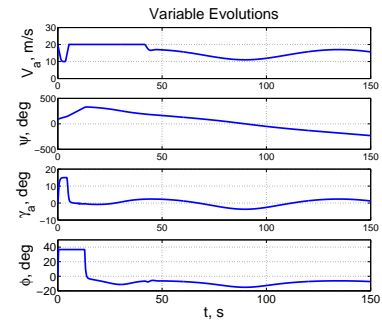
(a) 3-D view of system trajectory.



(b) Top-down view of system trajectory.



(c) Trajectory tracking errors.



(d) Evolution of the states.

Fig. 6: Simulation results using dynamic model.